Supporting Information

Kriegler et al. 10.1073/pnas.0809117106

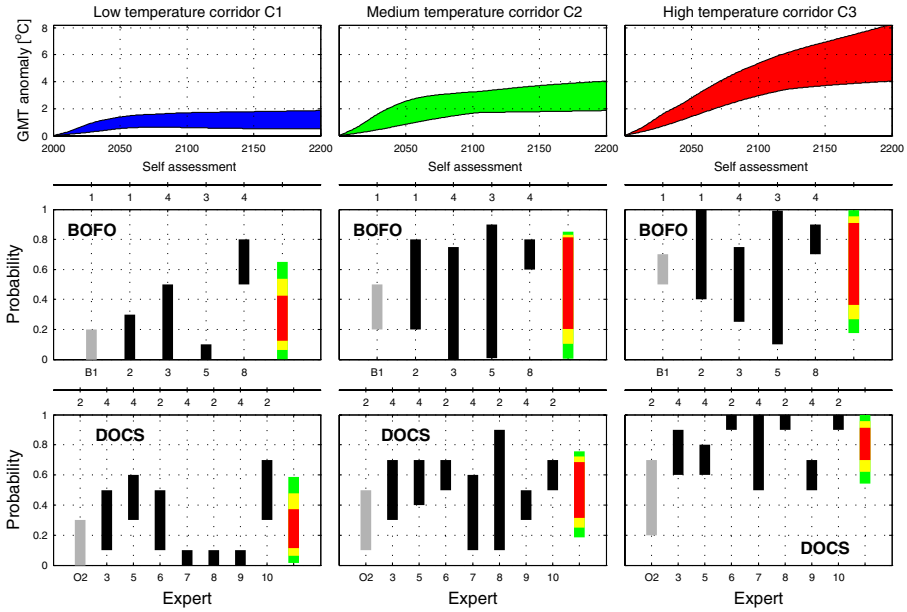

Fig. S1. Probability intervals from experts for BOFO and DOCS conditional on 3 different corridors for future global mean temperature (GMT) increase until 2200 (relative to year 2000 temperatures, see top row). The presentation of expert opinions has been anonymized by labeling a random permutation of experts with numbers (shown below each panel). Labels are tipping point specific as indicated by the preceding letters B, O. The self-assessment of experts is shown above each panel. Probability estimates of core experts (see text for an explanation) are depicted in black, while the remaining estimates are shown in gray. The rightmost bar in each panel shows the aggregation of probability intervals from core experts based on increasingly restrictive assumptions about expert weights: weights are allowed to vary by (*i*) $\pm 100\%$ (green) or (*ii*) $\pm 50\%$ (yellow) around uniform weights; (*iii*) average of lower respectively upper expert bounds (red). The increasing strength of assumptions leads to nested probability intervals (Red $<$ Yellow $<$ Green).

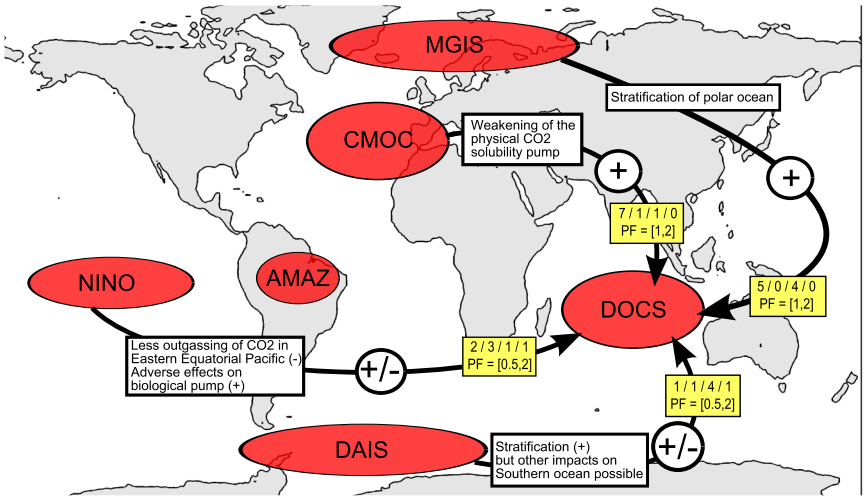

Fig. S2. Sketch of the main effects of CMOC, MGIS, DAIS, AMAZ, NINO on DOCS as described by participating experts. See Fig. 2 in the main text for remaining interactions among the first 5 tipping points. Pairs of tipping events *A*, *B* are connected with a directed arrow $A \rightarrow B$ if (*i*) at least 4 experts judged that some effect of triggering *A* on the probability of triggering *B* exists and (*ii*) they outnumbered the experts who saw no effect of *A* on *B*. Each arrow is accompanied by information about (*i*) whether the majority of those experts identified an increase (+), decrease (−), or uncertainty in the direction (±) of the probability of triggering *B* after *A* occurred (white circles), (*ii*) the number of experts supporting an increase/decrease/uncertain direction/no effect (top line, yellow boxes), (*iii*) the range of factors *PF* by which the probability of triggering *B* is believed to change after *A* occurred (union of *PF* intervals from only those experts that provided estimates in accordance with the type of effect attributed to each arrow; yellow boxes, bottom line), (*iv*) the dominant physical mechanism(s) described by some of the experts (white rectangles).

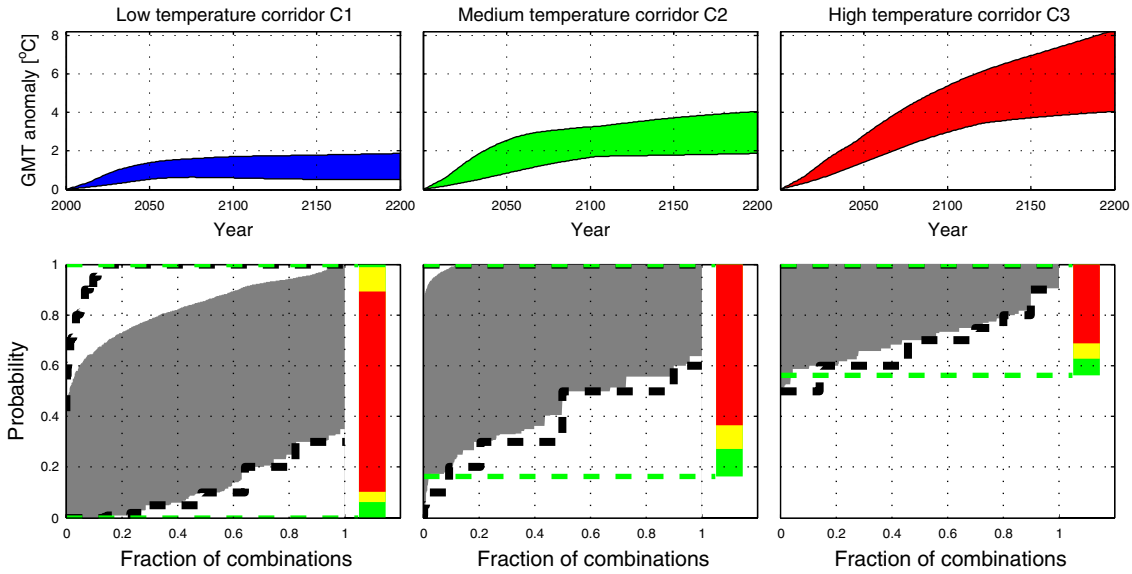

Fig. S3. Range of probabilities that at least 1 tipping point (among CMOC, MGIS, DAIS, AMAZ, NINO) is triggered conditional on the temperature corridors depicted in the upper row. The lower row shows increases of lower and upper probability bounds (encompassing the gray area) as a function of the 56,160 possible combinations of interval estimates for the marginal probability of triggering the individual tipping points given by core experts (i.e., as a function of the fraction of combinations for which the bound is lower or equal to the plotted value). The colored bars to the right show the probability ranges resulting from the combination of linearly pooled marginal probability intervals (Fig. 1, rightmost bars; see caption for the relation between color code and aggregation procedure.) The case of imprecise linear pooling with ± 100% variations of expert weights around uniform weights (green) describes a probability range (between green dashed lines) encompassing 96–100% of results from combination of individual expert estimates. All probability bounds discussed so far include the assessment of interactions between tipping points depicted in Fig. 2. Black dashed lines show the outer approximation of the probability range by Fréchet bounds that disregard any (in)dependency information between tipping points. See *SI Appendix* 1, Section 4 for further explanation.

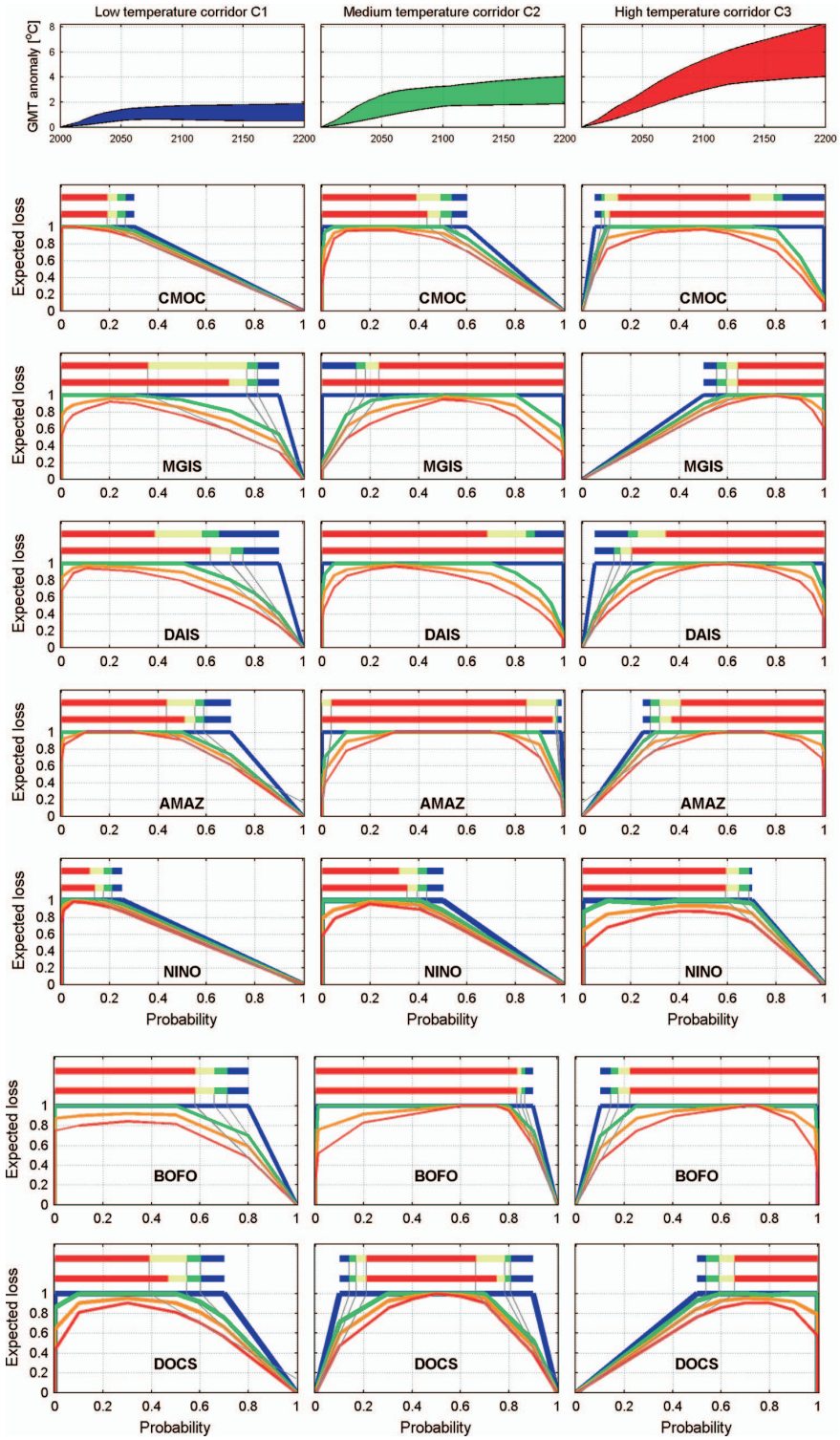

Fig. S4. Application of Nau's pooling rule (see *SI Appendix* 1, Section 3) to the aggregation of expert estimates for all tipping points (one per row). Shown are the pooled Bayes' risk functions conditional on 3 GMT corridors (Upper row) under 4 different assumptions on the uncertainty about expert weights: (*i*) uniform weights with no uncertainty (red), ±50% variations around uniform weights (orange), ±100% variations around uniform weights (green), and complete ignorance about expert weights (blue). The 2 horizontal bars on top of the Bayes' risk functions show the corresponding probability intervals of triggering a tipping point at 100% confidence level (outer bounds, lower bar) and 80% confidence level (upper bar). The color coding corresponds to the choice of uncertainty about expert weights (see above; orange Bayes' risk functions correspond to yellow intervals). Thin gray lines illustrate the derivation of these intervals from the risk functions. The illustration for CMOC, DAIS, NINO, BOFO refers to the intervals at 100% confidence level, and for MGIS, AMAZ, DOCS to the intervals at 80% confidence level.

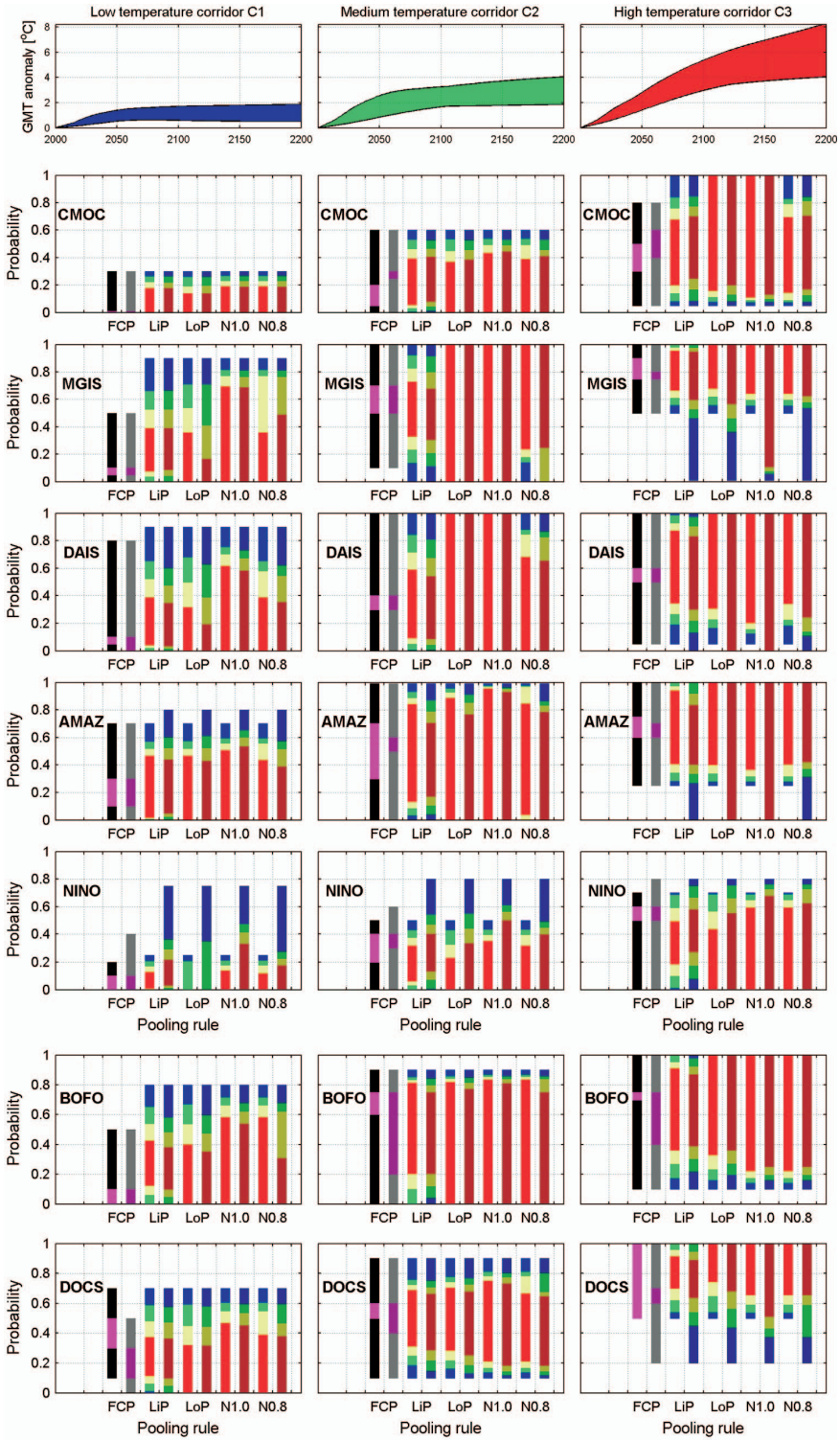

Fig. S5. Comparison of probability intervals from various pooling rules for all tipping points (1 per row). Shown are the pooled probability interval of triggering a tipping point conditional on 3 GMT corridors (upper row) from (*i*) forced consensus pooling (FCP; union of intervals: gray/black, intersection of intervals: pink/magenta), (*ii*) linear pooling (LiP), (*iii*) logarithmic pooling (LoP), (*iv*) Nau's pooling at 100% confidence level (N1.0), and (*v*) Nau's pooling at 80% confidence level (N0.8; see *SI Appendix* 1, Section 3 for details on the pooling rules). For each pooling rule, results are depicted for (*i*) the opinion pool containing only core experts (left bar; bright colors) and (*ii*) the opinion pool containing all experts (right bar; darkened colors). For LiP, LoP, N1.0, and N0.8, probability intervals depend on the choice of uncertainty about the distribution of expert weights: (*i*) uniform weights with no uncertainty (red), ±50% variations around uniform weights (yellow), ±100% variations around uniform weights (green), and complete ignorance about expert weights (blue).

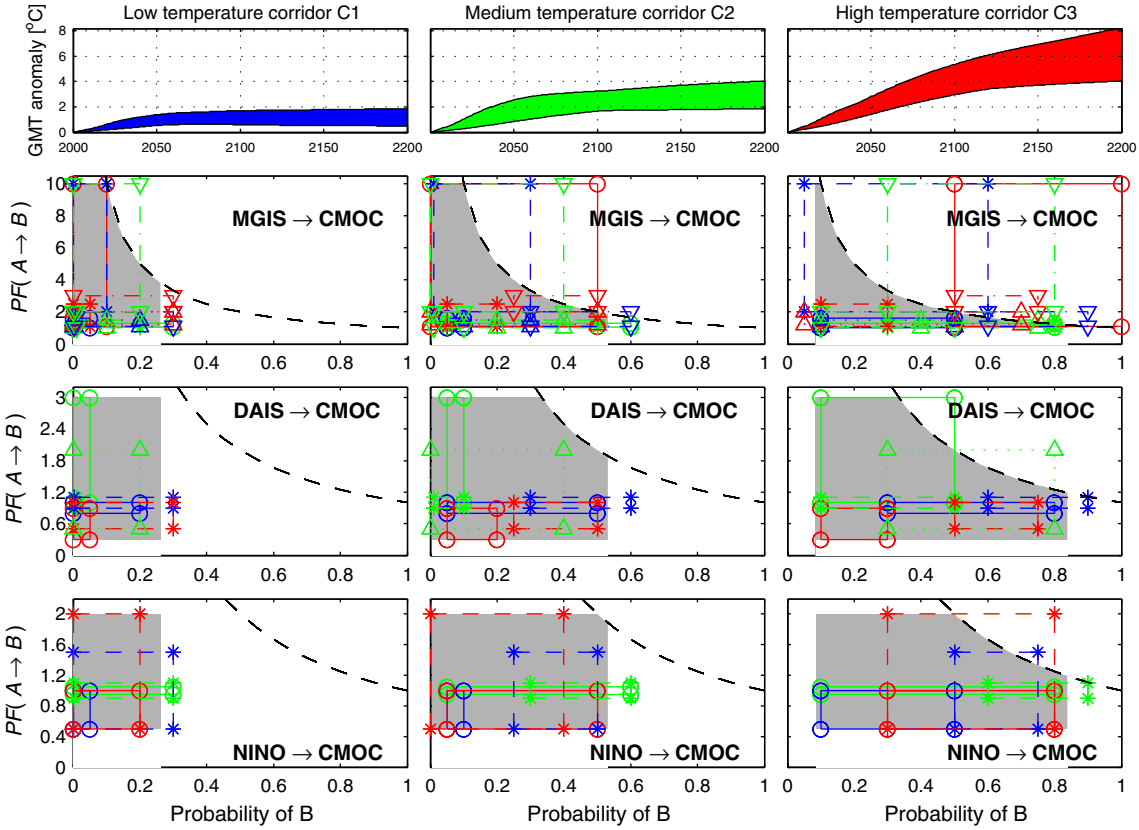

Fig. S6. Joint presentation of bounds on (*i*) the marginal probability of triggering a tipping point *B* (*P*(*B*) on the abscissa) and (*ii*) the ratio of the probability of triggering *B* given that *A* has been triggered before *B* to the marginal probability of triggering *B* (*PF*(*A* → *B*) on the ordinate) for effects of (*i*) MGIS, DAIS, NINO on CMOC, (*ii*) CMOC, NINO on AMAZ, (*iii*) CMOC, AMAZ on NINO, (*iv*) CMOC, DAIS on MGIS, (*v*) CMOC, MGIS, NINO on DAIS. Shown are estimates from only those experts who specified bounds on both quantities, constituting only a subset of those experts who specified bounds on *P*(*B*). Each expert estimate is shown by a colored rectangle. Note that the bounds on *P*(*B*), but not the bounds on *PF*(*A* → *B*), are dependent on the corridor for GMT increase (upper row). The curved dashed lines depict the absolute upper bound on *PF*(*A* → *B*), given by 1/*P*(*B*). Shaded areas provide an example of aggregated bounds that have been considered to calculate the lower and upper probability for triggering at least 1 of the 5 tipping points CMOC, MGIS, DAIS, AMAZ and NINO. See *SI Appendix* 1, Section 4 for further details.

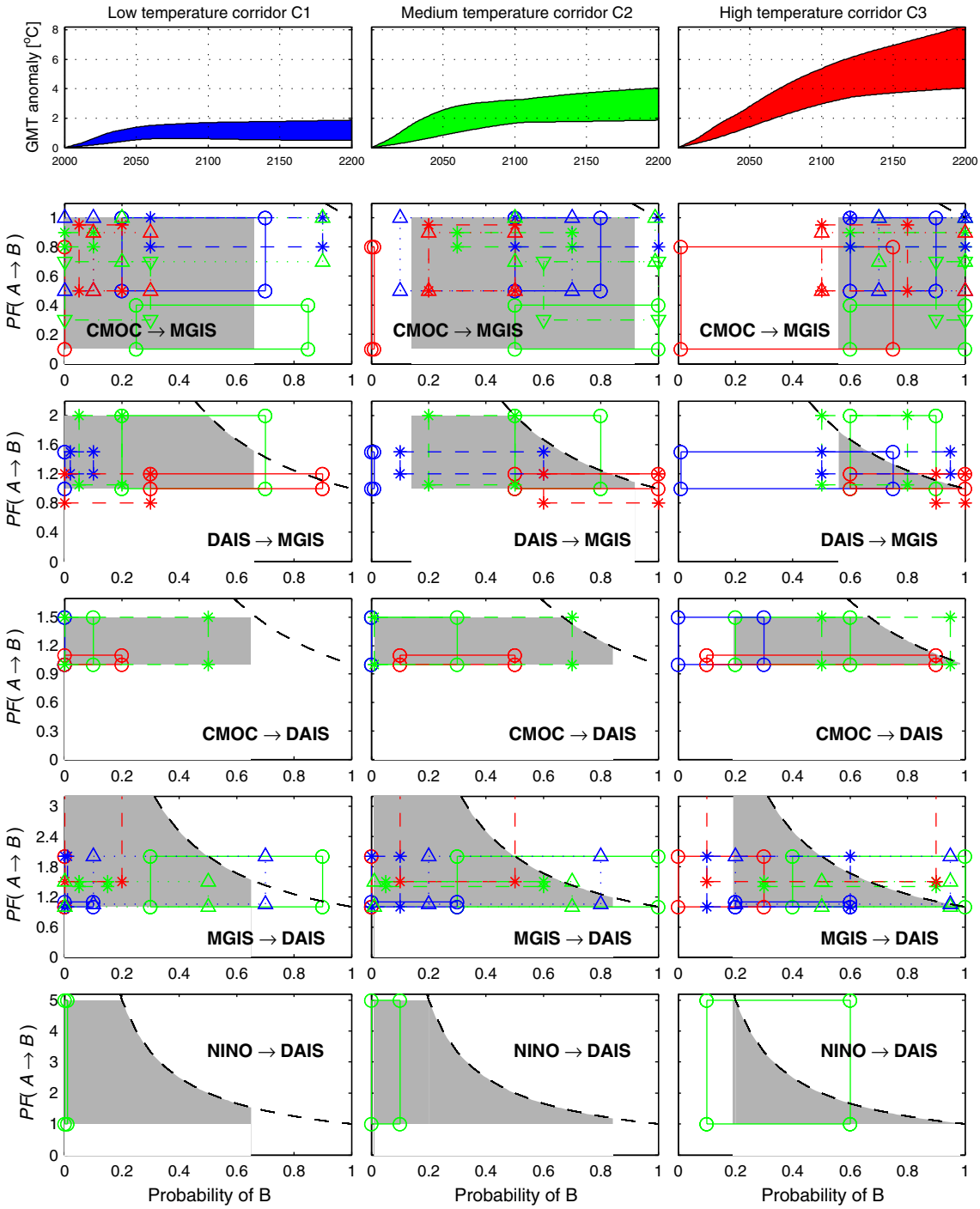

Fig. S6. (continued).

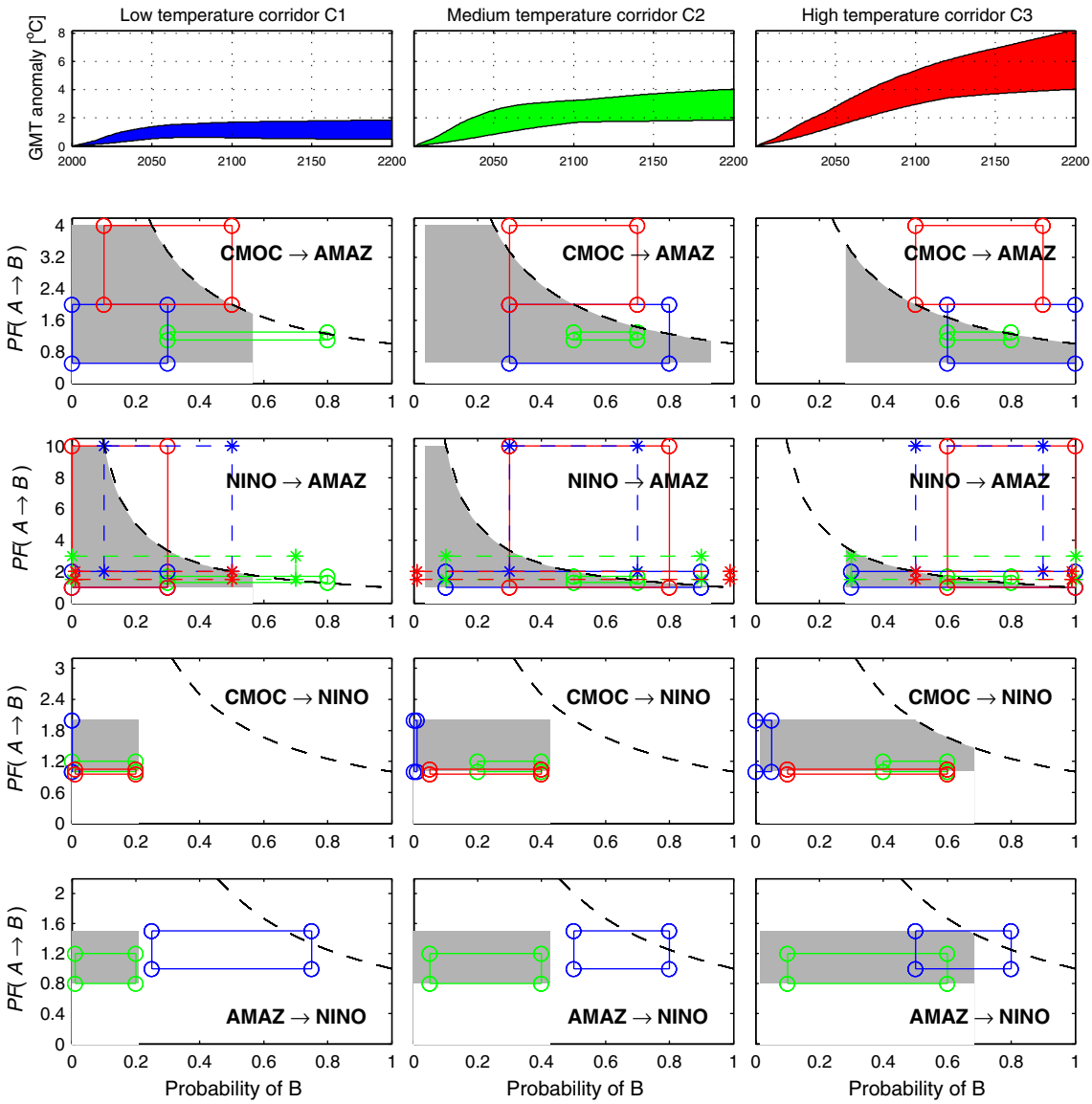

Fig. S6. (continued).

Other Supporting Information Files

SI Appendix
Table S1
Table S2
Table S3